Evaluation and possible direct utilization of low- to medium-enthalpy geothermal resources for the sustainable development of the African continent

Claudio Zuffi[a-b], Luca Socci[a], Andrea Rocchetti[a], Giampaolo Manfrida[a] and Daniele Fiaschi[a]

[a] Department of Industrial Engineering, University of Florence (Italy),
[b] claudio.zuffi@unifi.it, CA

Abstract:

Low- and high-enthalpy geothermal resources exist throughout the African continent, but their utilization is still minimal. The rift valley area includes several high-enthalpy resource manifestations, but numerous medium- and low-enthalpy resources characterize the mainland. Geothermal resources offer a large energy potential suitable for several users. The main goal of this article is the assessment of the energy potential of the geothermal resources in Africa for direct use. The analysis of different types of medium- and low-enthalpy resources is carried out. The use of absorption cycles for cold production is considered here. A parametric analysis of the resource conditions, with special reference to the temperature level, allowed the estimation of the cooling power potential connected to the low to medium geothermal energy resources available in the African continent. On the other hand, possible end users of this resource are identified cold room storage and building cooling. The present study covers several aspects, from thermodynamic modelling to environmental analysis. The mathematical model allows the simulation of the cooling system and, through parametric analyses, the most suitable cycle characteristics are determined in compliance with the potential of the available geothermal resource. The Life Cycle Assessment (LCA) methodology is adopted for the sustainability analysis and the assessment of environmental compatibility of the proposed solutions. A parametric Life Cycle Inventory (LCI) is developed, modeling the components according to the required size for each use. The main outcome of the present work is that the low enthalpy Geothermal available in the African continent can offer significant energy savings and large environmental benefits, which may play a fundamental role in the sustainable development of this area.

Keywords:

Geothermal energy, direct use, Absorption Refrigeration System, Life Cycle Assessment

1. Introduction

Geothermal energy is acknowledged as a renewable source with a very relevant potential, and technologies to exploit it are at a rather advanced stage of development [1]. The use of this source is mainly classified into two categories: *indirect*, in which electricity is produced by power plants; direct, which directly exploits the geothermal heat flow for several applications, from residential to industrial heating [2]. Over the years, the installed geothermal powerplant capacity has grown extensively. In 2000, the worldwide installed capacity was 7.97 GWe producing about 49.30 GWh/y [3], while at 2020 the installed capacity had roughly doubled to 15.95 GWe producing about 95.10 GWh/y electricity [4]. The currently available technologies for electricity production are dry steam, flash steam and binary cycles, usually for medium-high enthalpy resources ranging from 120° C to 350° C. On the other hand, in a 20 years range period, the direct use of the resource has also grown extensively, from 15.14 GWt in 2000 to 107.73 GWt in 2020 installed capacity, with a growth in the produced heat from 1.9E+5 TJ/y to 1.02E+6 TJ/y at worldwide level [5]. The direct heat uses can vary widely, often involving space heating and cooling for building or industrial applications: Heat pumps, Heat Exchangers, Absorption cooling and refrigeration, greenhouses, agricultural drying, fish farming and others. The choice is highly related to the temperature level of the resource and to that required for the specific applications [6]. Generally, the direct heat use technologies belong to medium-low enthalpy resources, usually ranging between 20° C and 150° C.

The African continent, and in particular the East Area where Rift valley is located, has a very high geothermal potential (over 15 GW) but the exploitation of this resource is still limited to extremely low fractions [7]. In 2020, data on the installed geothermal power in Africa amounted to 830 MWe, of which 823 MW in Kenya and 7 MW in Ethiopia. On the other hand, direct use of geothermal heat in the African continent is about 198 MWt, shared between several countries. Direct use applications are more equally distributed across the entire continent (Algeria, Burundi, Egypt, Ethiopia, Kenya, Madagascar, Malawi, Morocco, Nigeria, South Africa and Tunisia) [5].

In this context, investigating direct-use applications of geothermal heat for low to medium-enthalpy resources in the African scenario is of relevant interest. In the 40 – 150 °C heat range, the Absorption Refrigeration System (ARS) is economically and environmentally promising [8]. Several studies were conducted considering different conditions of the geothermal resource. Tugcu et al. analysed an ARS with ammonia-water mixture fed by a geothermal resource at 133°C [9]; Kairouani et al. evaluated an ARS with a mixture of ammonia and water and the geothermal resource in a range between 72°C and 75°C [10]; Velàzquez et al. have designed a single- and double-effect ARS which utilises a geothermal resource at 80°C and 163°C respectively [11].

Similarly, some paper in literature analyse the sustainability of geothermal heat for refrigeration and chilling, evaluating the coupling of the generator to different renewable sources with the Life Cycle Assessment methodology. Solano-Olivares et al. and Bukoski et al. evaluated an absorption cycle coupled with a solar system for building cooling [12], [13]. Hamedani et al. analysed the energy and environmental aspects through LCA of a biomass-fuelled heating and cooling system [14]. On the other hand, Maione et al. and Chaiyat, assessed the environmental impacts of coupling the ARS to a geothermal resource [15], [16].

In numerous regions of Africa, electricity is not easily accessible and distributed. As a result, geothermal energy plays a crucial role in the country's development. Thus, investigating systems that harness the existing heat from geothermal resources facilitates the implementation of multiple systems that would be considerably more challenging if powered by electricity. The objective of this work is modelling and evaluating the thermodynamic behaviour and the environmental impact of an ARS for different possible geothermal conditions. It is designed to cover the cooling load of a cold room (for food storage or other industrial use) or a building. The thermodynamic performance of an absorption cycle with a mixture of water and ammonia under different geothermal resource conditions have been evaluated. At the same time, the environmental impact assessment of the investigated ARS has been carried out by the means of Life Cycle Assessment (LCA), considering the construction and operation phase of the system.

This work is done in the framework of the European Horizon 2020 project Long-Term Joint EU-AU Research and Innovation Partnership on Renewable Energy *(LEAP-RE)* [17].

2. Materials and methods

The analysed ARS is an absorption cycle with a mixture of water and ammonia (NH_3/H_2O mixture) for the refrigeration of a cold room or cooling of a building. The proposed mathematical model of the ARS takes into account the chemical characterization of the mixture, the mass and energy balances. In order to realize a model suitable and easily applicable to different conditions of the African continent, several wide range variable parameters were considered. The parametric analyses focused on condensation temperature (T_{cond}), evaporation temperature (T_{evap}), mass ratio of NH_3 to the whole mixture (y), and finally the temperature of the geothermal resource (T_{geo}).

An environmental analysis was performed by the Life Cycle Assessment of the ARS, following the ISO 14040 and ISO 14044 standards [18], [19] The regulations define 4 key steps in this analysis: Goal and scope definition, Life Cycle Inventory (LCI), Life Cycle Impact Assessment (LCIA), Interpretation. In this work, the focus was on the second step, consisting in the development of a parametric LCI representing the construction phase of the absorption cycle. The goal is to provide the assessment of materials needed for construction in relation to the cooling power of the ARS, refereed to the installed kW unit. In addition, some parameters used in the thermodynamic model are set to evaluate the operation phase as well. Then, by combining the results obtained from the thermodynamic model and using them as inputs of the LCA model, it is possible to perform a comprehensive analysis of system performance and sustainability. This is done by varying the external conditions such as outdoor temperatures T_{air}, and target temperatures T_{aim}. The next sections describe the thermodynamic model and the LCA model of the considered plant, outlined in Figure 1.

The mathematical model of the absorption cycle was implemented in Engineering Equation Solver (EES) software [20], whereas the environmental analysis was conducted with OpenLCA software [21] and Ecoinvent 3.7 datatbase [22].

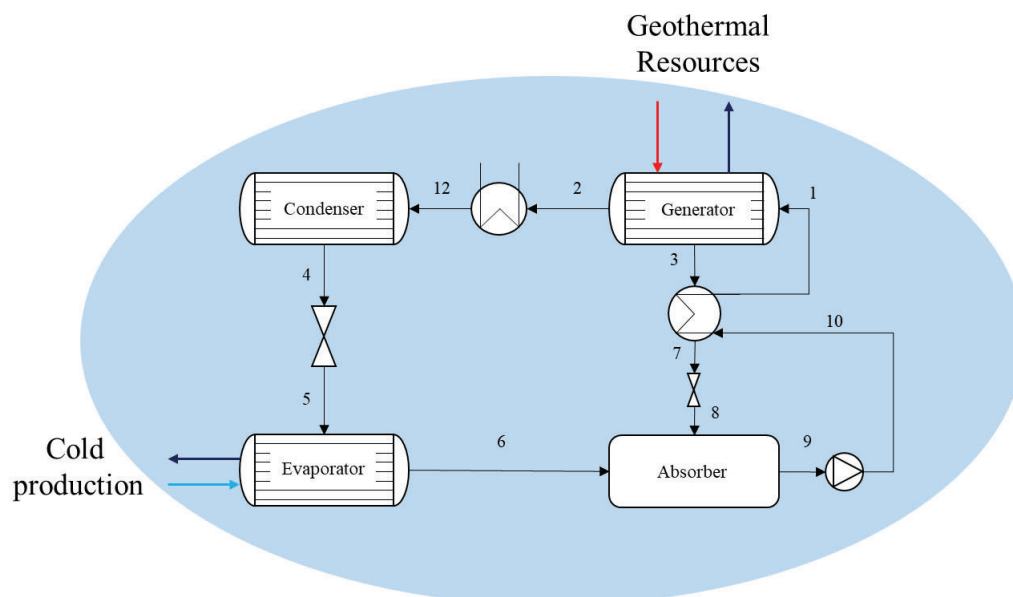Figure 1 - Geothermal absorption cycle for refrigeration, with a mixture of water and ammonia

2.1 Energy modelling

The ARS is a single-effect cycle, mainly consisting of generator, desuperheater (DSH), condenser, evaporator, absorber, and heat recovery unit (RH). The system is shifted in two lines, differently modelled according to the working fluid. At the generator outlet, from point 2 to point 6, the working fluid is pure ammonia starting as superheated vapor in 2, saturated vapor in 12, saturated liquid in 4 and saturated vapor in 6. From the generator outlet at point 3 (line 3-8) and the absorber outlet at point 9 (line 9-1) the working fluid is in the liquid state, consisting in a mixture of NH_3/H_2O at the concentration y. The working fluid is at a high concentration y in line 9-1 (strong solution), corresponding to the design concentration of the cycle, and at low concentration

in line 3-8. With reference to the external conditions, two parameters mainly influence the cycle, namely the temperatures at point 4 (T_{cond}) and the NH_3 mass ration at point 9 (y), as they set the two pressure levels of the cycle:

- High pressure corresponding to the saturation pressure of ammonia at T_{cond};
- Low pressure corresponding to the saturation pressure of the mixture evaluated at temperature T_{cond} with mass ratio y.

T_{cond} is determined by the external conditions (1), hence the environmental air temperature, while y is set and evaluated at different level. The reason for setting the temperature T_9 equal to the temperature T_{cond} is that the absorber exchanges heat with the outside air. T_{evap} is evaluated from the low-pressure level as the saturation temperature at low pressure and also defines the aim temperature (T_{aim}) achievable in the cold room or in the building (e.g. cold utility temperature) (2). Thus, these parameters uniquely set the cycle and a changing one of them leads to a variation in temperatures and pressures of the other components (Figure 2 - Temperature-pressure graph with constant water-ammonia concentration curves of the Absorption Refrigeration System), as will be seen in the Results section.

$$T_{cond} = T_{air} + \Delta T_{cond} \tag{1}$$
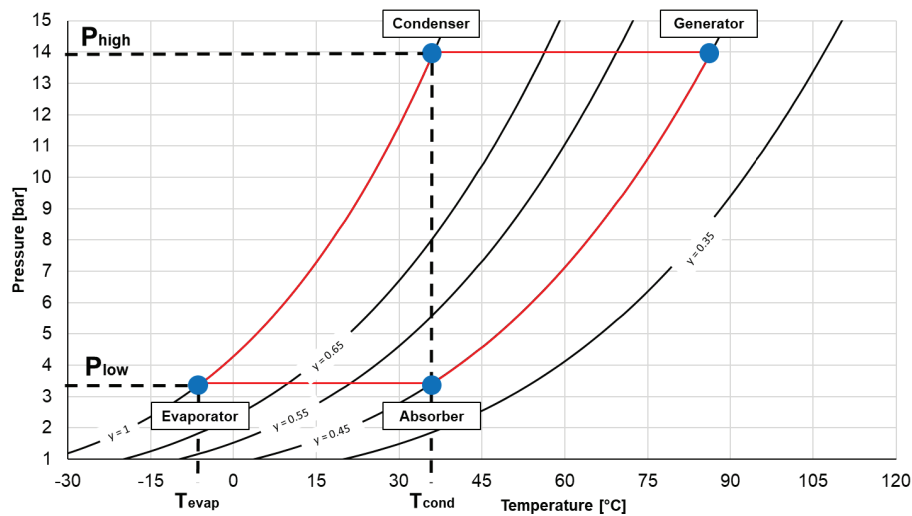
$$T_{evap} = T_{aim} + \Delta T_{evap} \tag{2}$$

Figure 2 - Temperature-pressure graph with constant water-ammonia concentration curves of the Absorption Refrigeration System

The whole cycle is calculated around these two fixed pressure levels. In Point 1, the water-ammonia mixture enters into the generator, which is heated by the geothermal resource. The temperature level at the generator output (point 3) is evaluated according to equation (3), where T_{geo} is the temperature of the geothermal resource entering the generator.

$$T_2 = T_3 = T_{geo} - \Delta T_{gen} \tag{3}$$

Thus, from point 2 the ammonia in the superheated vapour state passes through the desuperheater (DSH) and successively condenses at point 4. Downstream the isenthalpic throttling valve (4-5), the ammonia evaporates into the evaporator (5-6), providing the required refrigeration effect. At the same time, in point 3 the weak water / ammonia solution under the liquid state releases heat (thus recovered) to the NH_3/H_2O strong solution from the absorber. The regeneration level R of this recuperator is defined in equation (4).

$$R = (h_3 - h_7) \Big/ (h_1 - h_{10}) \tag{4}$$

The equations governing the energy balances of the main points of the cycle are given below from (5 to 14).

$$Q_{geo} = \dot{m}_{geo} * (h_{15} - h_{16}) \tag{5}$$

$$Q_{geo} = \dot{m}_2 * h_2 + \dot{m}_3 * h_3 - \dot{m}_1 * h_1 \tag{6}$$

$$Q_{DSH} = \dot{m}_2 * (h_{12} - h_2) \tag{7}$$

$$Q_{cond} = \dot{m}_2 * (h_{12} - h_4) \tag{8}$$

$$Q_{evap} = \dot{m}_2 * (h_4 - h_6) \tag{9}$$

$$Q_{abs} = \dot{m}_2 * h_6 + \dot{m}_3 * h_8 - \dot{m}_1 * h_9 \tag{10}$$

$$\dot{m}_1 * (h_1 - h_{10}) = \dot{m}_3 * (h_3 - h_7) \tag{11}$$

$$Q_{abs} = \dot{m}_2 * h_6 + \dot{m}_3 * h_8 - \dot{m}_1 * h_9 \tag{12}$$

$$W_p = \dot{m}_1 * (h_{10} - h_9) \tag{13}$$

$$COP = Q_{evap} \Big/ (Q_{geo} + W_p) \tag{14}$$

The model relies on some fixed parameters set during the analysis, while other ones are allowed to vary. Table 1 shows all fixed and variable parameters and their values or ranges. T_{cond} and T_{evap} are evaluated to analyse their influence on the Coefficient of Performance (COP) of the whole system. The sensitivity analysis to the NH3/H2O solution concentration y is carried out to determine the most suitable ammonia concentration for the cycle in relationship to the available low-temperature level of the geothermal resources. Finally, T_{geo} allows defining the performance level achievable referred to the heat input to the system.

Table 1 - Range of parameters used in the parametric analysis of the system

Name	Parameter	Unit	Value /range
Hot-cold side temperature difference at the condenser	ΔT_{cond}	°C	10
Hot-cold side temperature difference at the evaporator	ΔT_{evap}	°C	5
Hot-cold side temperature difference at the generator	ΔT_{geo}	°C	5
RH regeneration level	R	-	0.8
Condenser temperature	T_{cond}	°C	25 – 50
Evaporator temperature	T_{evap}	°C	-10 – 0
Mass fraction Ammonia/mixture	y	kg $_{NH3}$/kg $_{mixture}$	0.3 – 0.8
Geothermal mass flow rate	m_{geo}	kg/s	0.5 – 10
Temperature of resources	T_{geo}	°C	50 – 120

2.2 LCA Modelling

The surface plant for refrigeration defines the system boundaries of the analysis. Geothermal wells or the drawdown point are not considered because they are strongly site dependent. The cold room or the building are as well not considered at the analysis, as out of the focus of this work. The electricity consumption of the pumps is taken into account, and it's impact is modelled using Kenya's electricity energy mix as a reference. The assumed functional unit is 1 kW of installed cooling power.

The parametric LCI consisted in two basic steps:

- Finding a reference process representative of the construction materials of the absorption cycle;
- Finding enough data to establish a relationship between the installed cooling capacity and the weight of the device.

For the first step, a literature review was conducted, and several LCIs were compared [12]–[16]. It turned out that many of them were either incomplete or referred directly to secondary processes in the database. For this reason, to consider a consistent reference, the process of the Absorption cycle provided by the Ecoinvent 3.7 database [22] was adopted as a reference model. This process was the starting point to obtain the typical composition of materials for the devices of the case study. Indeed, by neglecting the materials not closely related to the construction phase of the devices, a relative mass fraction (%) of construction materials was made per each considered unit. The second step was finding reliable catalogues of Absorber manufacturing companies. The purpose of this step is achieving information on weight and cooling power. Once obtained the necessary data, a distribution of points outlining the relationship between the weight of the devices and the nominal ARS cooling power (kW) may be traced. The *World Energy Absorption Chillers Europe Ltd* catalogues available online[23] were used which allowed to obtain 140 number of points.

With the distribution of this data in hands, it was possible to achieve a satisfactory second-degree polynomial fitting function. The second-degree function was selected in order to limit its complexity, increasing with the polynomial degree, without entailing an appreciable reduction of the uncertainty. Figure 3 shows the point distribution and the related 2nd degree polynomial power-weight fitting function.

$$y = 5E\text{-}07x^2 + 0.0092x + 1.5237$$
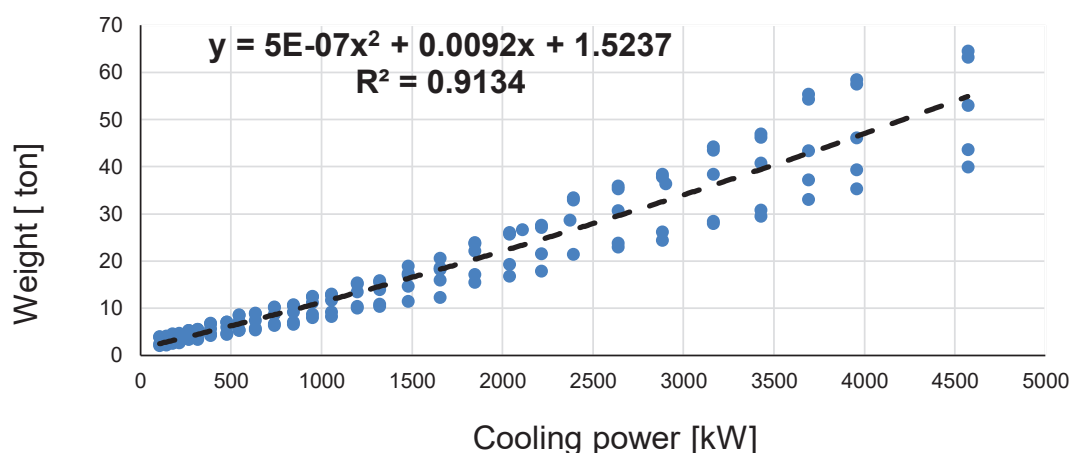$$R^2 = 0.9134$$

Figure 3 - Descriptive function of installed cooling power-weight trend

The conducted analysis adopts the Environmental Footprint (EF) 3.0 methodology, adapted to the Ecoinvent database. Specifically, the analysis develops on two levels: (i) Analysis of the environmental indicator Climate Change (CC) in terms of kg CO_2 equivalent emitted and (ii) analysis of the single score in terms of Environmental Points (Pt). The latter is achieved following normalization and weighting of all indicators evaluated by EF3.0, therefore it represents the overall environmental impact of the system.

3. Results

In this section, the results coming from energy parametric analysis and LCA study are presented. In particular:

- The parametric analysis shows the sensitivity of the absorption refrigeration cycle to the ammonia concentration in the mixture, condensation temperature and geothermal resource temperature.
- The LCA study shows the contributions analysis of the environmental indicator Climate Change (CC), as well as an analysis of the most impactful categories at single score level.

3.1 Effect of ammonia concentration

Figure 4 shows the temperature trend of the NH_3/H_2O mixture at the generator inlet T_1 and the evaporation temperature T_{evap} with respect to different y_1 levels. In this case, the analysis was carried out by keeping the T_{geo} set at different temperature levels: a) 120°C; b) 100°C; c) 80°C; d) 60°C. The y analysis highlights a key aspect of low-, and medium-enthalpy geothermal resources and the target temperature. The first aspect that results is that as y_1 increases, the temperature T_1 decreases and T_{evap} increases. Respecting the constant

concentration curves of the ammonia-water mixture shown in Figure 2, it is denoted that as the selected curve in the Aborber-Generator stream varies, the temperature levels at the generator and evaporator also vary.

This means that increasing y_1 allows geothermal resources to be exploited at lower temperatures. However, it must be considered that the refrigeration effect for cold room can be obtained at most for T_{evap} in the order of 5°C while, for the cooling of a building, T_{evap} must be higher than this level. As a reference, it must be considered that a satisfying refrigeration effect for a cold room can be obtained for T_{evap} not higher of 5°C (while, for the cooling of a building, Tevap could be higher). Taking this graph into account, it is easy to identify the NH_3/H_2O concentration y_1 which allows the required performance to be obtained with respect to the temperature of the geothermal resource. There is a grey area in the graphs, the low side of this area represents the temperature level of geothermal resource. This implies that the T_1 profile is not acceptable when it crosses this area and it can only assume values below that level. For low-temperature resources, the variation of y_1 is very limited and therefore also the terminal uses forcing only one type of application such as the cooling of buildings. Conversely, for higher temperature levels, such as a) and b), it is possible to choose both applications of cold storage and building cooling.
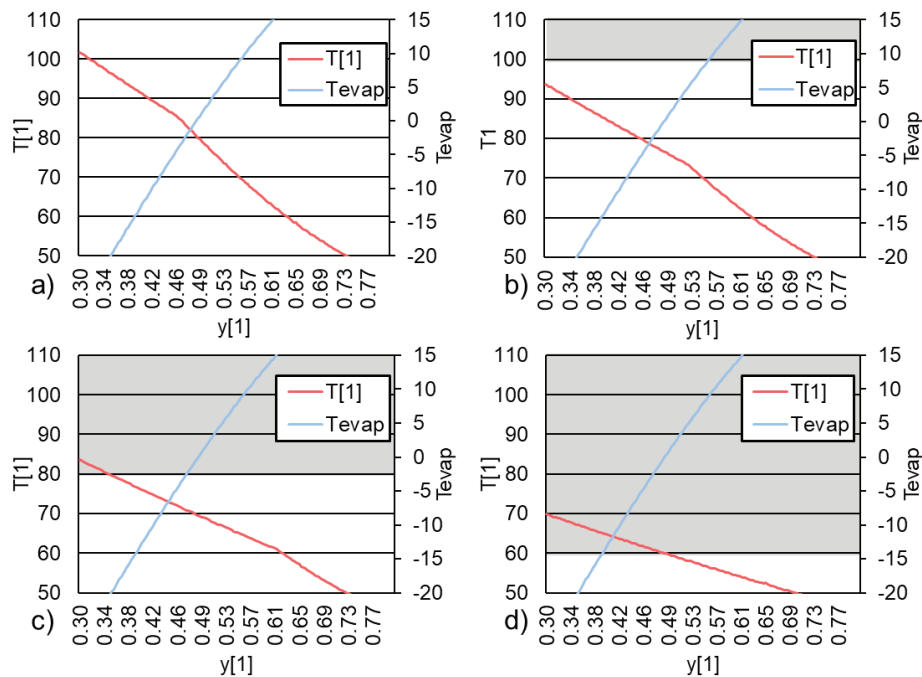

Figure 4 - Parametric analysis of T_1 and T_{evap} as a function of y_1 at different level of T_{geo}: a) T_{geo} =120°C; b) T_{geo} = 100°C; c) T_{geo} = 80°C; d) T_{geo} = 60°C.

3.2 Effects of condensation temperature

Through the parametric analysis of T_{cond}, the trend of the system's COP)is investigated using a function that is also dependent on y_1. In order to explore various T_{cond} variations, T_{geo} was set to its maximum level of 120°C. Figure 5 illustrates the relationship between COP and T_{cond} at different levels of y_1. It can be observed that at lower levels of y_1, higher COP values are achieved with lower T_{cond}, but as y_1 increases, the system's performance tends to decline.

However, for higher levels of y_1 ranging from 0.5 to 0.6, it appears that T_{cond} has minimal influence on COP. Since T_{cond} is influenced by external air temperatures, this indicates that these particular cases are minimally affected by external temperature changes, maintaining their performance almost unchanged within the typical temperature ranges of the African continent. Conversely, for cases where y_1 is below 0.45 to 0.35, variations in external temperatures significantly impact the system's performance, leading to a drastic drop in COP.

Another consideration is that the different y_1 levels correspond to a specific T_{evap} level, which are presented in Table 2. The cases relevant to refrigeration purposes focus on $y_1 = 0.5$. Realistically, considering the outdoor temperatures commonly encountered in East Africa, the design T_{cond} would fall within the range of 30-40°C [24], where the COP exhibits a declining phase. Furthermore, it should be noted that a slight increase in T_{evap} can slightly enhance the system's performance, but it may require applications beyond refrigeration, such as building cooling. Thus, considering all the aforementioned factors, the performance of the system is highly

dependent on its final application, as well as the external temperatures prevailing at the specific African site where the geothermal resource is located.
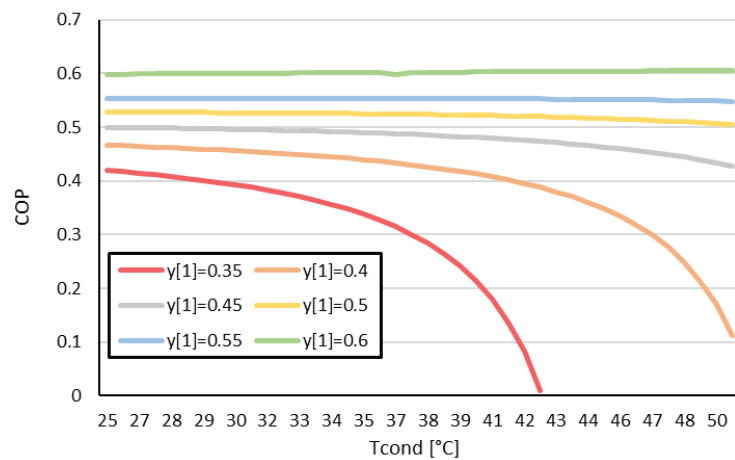

Figure 5 - Parametric analysis of COP as a function of T_{cond} and T_{evap}

3.3 Geothermal resource

The parametric analysis performed on the geothermal resource explores the trends of the COP at various y_1 levels. Figure 6 depicts the overall pattern, characterized by a substantial performance increase until reaching the temperature that maximizes COP, followed by a gradual decline. The lowest point of each curve corresponds to the geothermal resource temperature at which the absorption cycle initiates operation.

Considering the values presented in Table 2 and setting y_1 to 0.5 as the threshold for applications related to food refrigeration, it becomes evident that the minimum geothermal resource temperature is 83°C (lowest point of $y_1 = 0.5$ curve). As y_1 increases, corresponding to lower T_{evap} temperatures, the required geothermal resource temperature approaches the maximum value at a medium-low enthalpy level. In essence, lower y_1 levels in the cycle necessitate higher geothermal resource temperatures. This highlights the fact that refrigeration-type applications demand minimum temperatures around 80°C, which are only available in select regions of Africa, particularly in the East Africa Rift Valley (EARV) area.

Conversely, for higher y_1 levels, corresponding to higher Tevap temperatures, lower-temperature resources can be exploited, which are present in both the EARV and North Africa (e.g., Algeria and Morocco).

Hence, it is crucial to determine the optimal ammonia concentration, y_1, that maximizes COP as a function of the geothermal resource. For this reason, Table 2 provides the respective COP_{max} and T_{geo} values for each y_1 level.
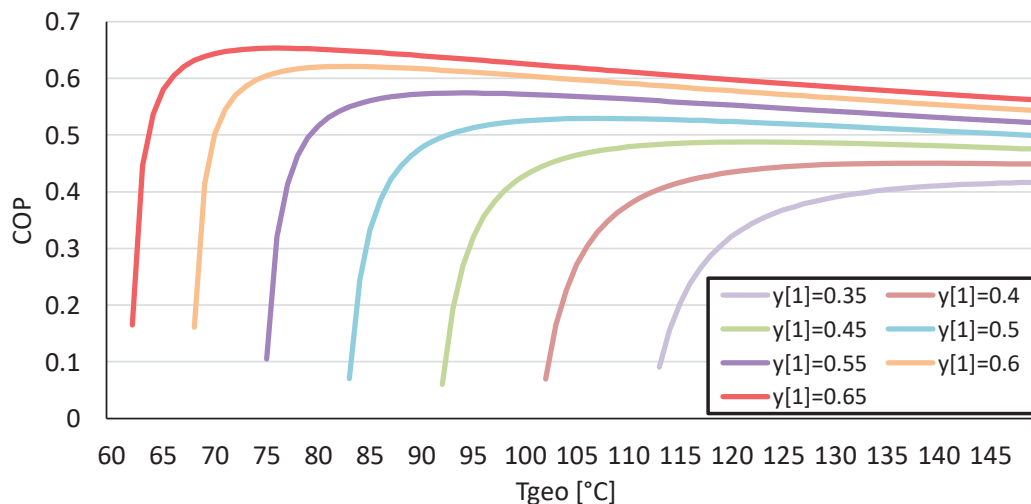

Figure 6 - Parametric analysis of COP as a function of T_{geo} and y_1

Table 2 - Evaluation of the maximum COP with respect to the temperature of the resource and the resulting cooling power

	y_1						
	0.35	0.40	0.45	0.50	0.55	0.60	0.65
T_{geo} [°C]	140	137	121	106	94	83	76
T_{evap} [°C]	-20.00	-12.56	-5.34	1.50	7.85	13.60	18.63
COP_{max}	0.41	0.45	0.48	0.52	0.57	0.62	0.65

3.4 Final application

Two cases are taken as reference: a) the first has the conditions set at y_1=0.5 and therefore T_{evap}=1.5° C for the refrigeration of a cold room for food storage purposes; b) the second has the conditions set at y_1=0.6 and therefore T_{evap}=13.60° C for the cooling of a building. In Figure 7 an analysis is shown on the heat loads of the main components, as the geothermal resource variations. As the two graphs show, for the cooling of the building it is possible to exploit a resource at temperatures above 70°C, while for the cold room it must be above 85°C. Analysing the point at which COP is maximum for both configurations show that for case a) the cold load is 21.34 kW while for load b) it is 22.27 kW.
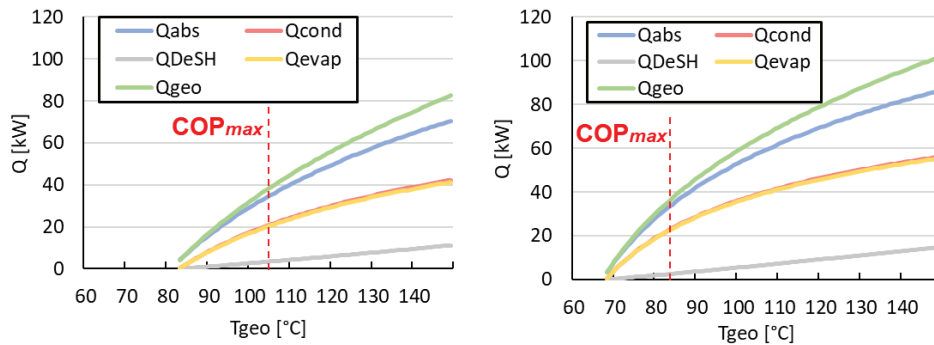

Figure 7 - Evaluation of heat level of two different cases: On the left a) for the application of a cold room, on the right b) for the cooling of a building

A preliminary dimensioning of a cold room was carried out to evaluate the output of the refrigeration and cooling system. Using equation 15 to estimate the annual cooling energy ($E_{cooling}$) in terms of kWh/y in a cold room for food storage. Where CF_a is the total number of hours per years of about 8000 [25], and F_r is a reduction factor of about 0.5. The results obtained for the reference case is approximately 85.360 MWh. Given data from literature 73 kWh/m^3 per year [26] for cold room is required, so a hypothetical cold room that is met by this system is 1169 m^3. At the same time, approximately 0.21kW/m^2 of cooling power is required for cooling a building with an internal temperature of 23°C [27]. Therefore, it can be estimated that with the analysed system a building of approximately 106 m^2 can be cooled. To make a point in support of these results, consider the case of the cold room. Taking as reference the results obtained from Evans et al. 2014 [28], an estimation can be made that suggests the consumption of around 56 kWh/m3 per year for cold room. It is crucial to emphasize that the availability of electricity poses challenges in numerous African regions, which underscores the necessity to devise a system that ensures access to electricity. In this context, the utilization of the geothermal resource in Africa assumes even greater significance.

$$E_{cooling} = Q_{evap} * CF_a * F_r \tag{15}$$

3.5 Life Cycle Impact Assessment

The analysis carried out on the environmental indicator CC, is shown in figure Figure 8. Here it is shown that the larger the installed cooling power of the device, the more CO_2 eq per kW of installed cooling power is reduced. In particular, the largest contribution of the impact comes from the electricity consumption of the operation phase, which is in the range of 60-65 % of the impact. In addition, the ammonia mixture makes a very low contribution ranging from 1.6-3.5 % of the impact. The construction phase results in approximately 1.94E+02-1.89E+021 kg CO2/kW, contributing 33-36% of the impacts.
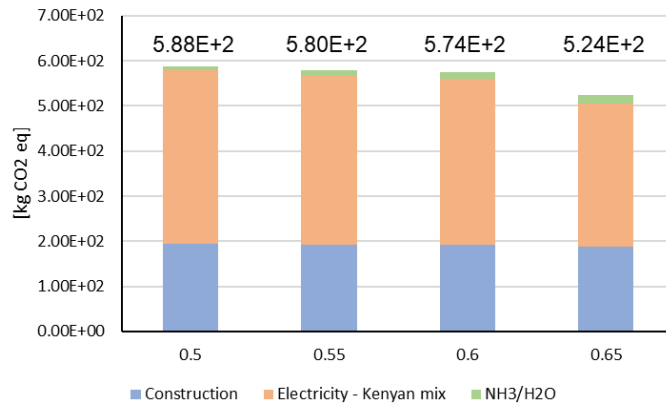

Figure 8 - Climate change evaluation

Finally, a single score analysis is shown in Figure 9, highlighting the contribution of the most impactful categories. The trend that was achieved for the CC indicator also persists at the overall system level. In fact, even at single score there is a decrease in impacts for systems with higher ammonia concentrations in the working fluid. Furthermore, globally, the most impactful categories are Resource use, minerals and metals, which impact in the range of 55-52%%. Two other indicators such as CC and Ecotoxicity, freshwater have a significant weight of about 9-11% and 11-12% respectively. While acidification, Particulate matter and Resource use, fossil impact about 3-6%, while the other indicators have negligible impact percentages.
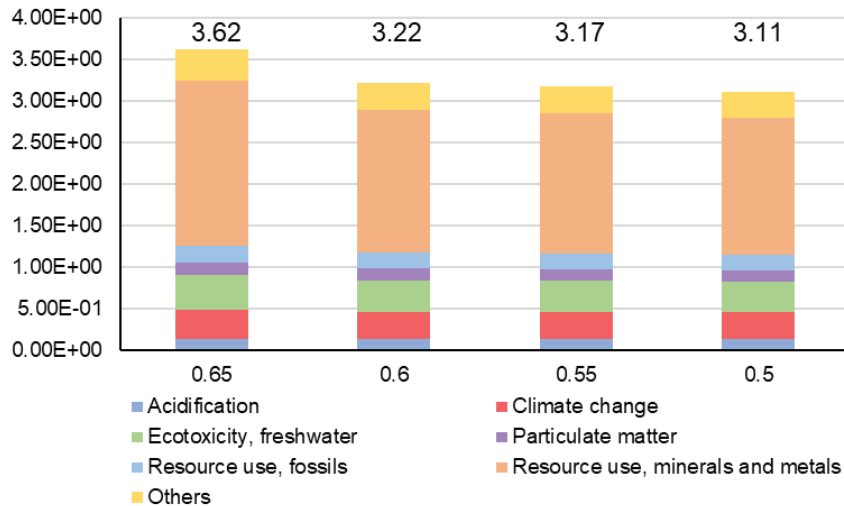

Figure 9 - Single score evaluation

4. Conclusion

In this paper, an application of direct use of the geothermal resource for medium and low enthalpy is analyzed. In particular, an absorption refrigeration system using a mixture of NH_3/H_2O is taken as a reference system for col room or building cooling. The analysis that has been conducted aims to highlight aspects concerning achievable thermodynamic performance and aspects concerning sustainability. For this reason, a thermodynamic model of the system was developed using the EES software to assess the performance of the cycle with several parametric analyses. From the analysis of the ammonia concentration, it can be deduced that increasing y_1 decreases the temperature of the mixture feeding the generator but at the same time increases the temperature level at the evaporator. This makes it possible to exploit a geothermal resource at a lower temperature but to increase the target temperature. The condenser temperature analysis shows that for low y_1, the increase in T_{cond} strongly reduces COP performance, whereas, for higher levels of y_1, the cycle is not influenced by these effects. The range of air temperatures in Africa limits T_{cond} to the 30-40°C range where the COP trend is decreasing. From the analysis of the geothermal resource, the minimum temperature values T_{geo} are set at different values of y_1. Furthermore, it is possible to evaluate the T_{geo} that maximizes the COP for each type of application. In particular, for refrigeration purposes, concentrations below 0.5 are required and COP_{max} is obtained for temperatures above 106°C. For the purposes of building cooling, on the other hand, y_1 greater than 0.55 is preferred and allows resources to be exploited at temperatures below 94°C. The results obtained dimension a cold room of 1169 m^3 at 5°C, using a resource at 106°C, and a building to be cooled of 106 m^2 at 23°C, with a resource at 86°C. To analyze the sustainability of the considered system, an LCA was conducted developing a parametric LCI to represent the construction and operation phase of the system. It was used OpenLCA software and the EF3.0 methodology adapted to the Ecoinvent 3.7 database. LCA uses the cooling power installed of the system as functional unit. Only the cooling system is analyzed, neglecting the entire system outside it (geothermal resource extraction point, cold room, building).

The outputs obtained from the thermodynamic model, in terms of cooling power, energy consumption, mass flow rate of ammonia mixture, are taking as input for the parametric LCI. The analysis of the environmental indicator CC shows a reduction in impacts corresponding to the increase in installed cold power of the system. The main contribution comes from electricity consumption and accounts for about 60-65%, while the construction phase of the device accounts for 33-36%. The single score analysis determines the same trend as for CC, and it is also established that the environmental indicator with the highest impact is Resource use, minerals and metals for about 52-55%. The environmental impact of CC accounts for 9-11%.

5. Bibliography

[1]   I. W. Johnston, G. A. Narsilio, and S. Colls, "Emerging geothermal energy technologies," *KSCE Journal of Civil Engineering*, vol. 15, no. 4, pp. 643–653, Apr. 2011, doi: 10.1007/s12205-011-0005-7.

[2]   M. T. Islam *et al.*, "Trends and prospects of geothermal energy as an alternative source of power: A comprehensive review," *Heliyon*, vol. 8, no. 12. Elsevier Ltd, Dec. 01, 2022. doi: 10.1016/j.heliyon.2022.e11836.

[3]   E. Barbier, "Geothermal energy technology and current status: an overview," 2002. [Online]. Available: www.elsevier.com/locate/rser

[4]   J. W. Lund, G. W. Huttrer, and A. N. Toth, "Characteristics and trends in geothermal development and use, 1995 to 2020," *Geothermics*, vol. 105, Nov. 2022, doi: 10.1016/j.geothermics.2022.102522.

[5]   J. W. Lund and A. N. Toth, "Direct utilization of geothermal energy 2020 worldwide review," *Geothermics*, vol. 90, Feb. 2021, doi: 10.1016/j.geothermics.2020.101915.

[6]   D. Moya, C. Aldás, and P. Kaparaju, "Geothermal energy: Power plant technology and direct heat applications," *Renewable and Sustainable Energy Reviews*, vol. 94. Elsevier Ltd, pp. 889–901, Oct. 01, 2018. doi: 10.1016/j.rser.2018.06.047.

[7]   E. Y. Kombe and J. Muguthu, "Geothermal Energy Development in East Africa: Barriers and Strategies," *Journal of Energy Research and Reviews*, vol. 2, no. 1, pp. 1–6, 2019, doi: 10.9734/JENRR/2019/45278.

[8]   A. Keçeciler, H. I. Acar, and A. Dogan, "Thermodynamic analysis of the absorption refrigeration system with geothermal energy: an experimental study," *Energy Conversion & Menagement*, vol. 41, pp. 37–48, 2000, [Online]. Available: www.elsevier.com/locate/enconman

[9]   A. Tugcu and O. Arslan, "Optimization of geothermal energy aided absorption refrigeration system—GAARS: A novel ANN-based approach," *Geothermics*, vol. 65, pp. 210–221, Jan. 2017, doi: 10.1016/j.geothermics.2016.10.004.

[10] L. Kairouani and E. Nehdi, "Cooling performance and energy saving of a compression-absorption refrigeration system assisted by geothermal energy," *Appl Therm Eng*, vol. 26, no. 2–3, pp. 288–294, Feb. 2006, doi: 10.1016/j.applthermaleng.2005.05.001.

[11] J. Saucedo-Velázquez, G. Gutiérrez-Urueta, A. Pacheco-Reyes, and W. Rivera, "Case study: Design of an absorption refrigeration system for milk preservation in Jalisco, Mexico," *Case Studies in Thermal Engineering*, vol. 44, p. 102866, Apr. 2023, doi: 10.1016/j.csite.2023.102866.

[12] K. Solano–Olivares *et al.*, "Life cycle assessment of a solar absorption air-conditioning system," *J Clean Prod*, vol. 240, Dec. 2019, doi: 10.1016/j.jclepro.2019.118206.

[13] J. Bukoski, S. H. Gheewala, A. Mui, M. Smead, and S. Chirarattananon, "The life cycle assessment of a solar-assisted absorption chilling system in Bangkok, Thailand," *Energy Build*, vol. 72, pp. 150–156, Apr. 2014, doi: 10.1016/j.enbuild.2013.12.034.

[14] S. Rajabi Hamedani, M. Villarini, V. Marcantonio, U. di Matteo, D. Monarca, and A. Colantoni, "Comparative energy and environmental analysis of different small-scale biomass-fueled CCHP systems," *Energy*, vol. 263, Jan. 2023, doi: 10.1016/j.energy.2022.125846.

[15] A. Maione, N. Massarotti, R. Santagata, and L. Vanoli, "Environmental assessment of a heating, cooling and electric energy grid from a geothermal source in Southern Italy," *J Clean Prod*, vol. 375, Nov. 2022, doi: 10.1016/j.jclepro.2022.134198.

[16] N. Chaiyat, "A multigeneration system of combined cooling, heating, and power (CCHP) for low-temperature geothermal system by using air cooling," *Thermal Science and Engineering Progress*, vol. 21, Mar. 2021, doi: 10.1016/j.tsep.2020.100786.

[17] Horizon 2020, "Long-Term Joint EU-AU Research and Innovation Partnership on Renewable Energy - LEAP-RE project," *European Commission*, 2021. https://www.leap-re.eu/project-context/ (accessed Mar. 20, 2023).

[18] International Organization for Standardization (ISO), "ISO 14040:2021—Environmental management — Life cycle assessment — Principles and framework. Environ. Manage.," *Geneva, Switzerland*, 2021.

[19] International Organization for Standardization (ISO), "ISO 14044:2021 Environmental management - Life cycle assessment - Requirements and guidelines. Environ. Manage.," *Geneva, Switzerland*, 2021.

[20] "EES: Engineering Equation Solver. http://www.fchart.com/."

[21] "OpenLCA: Open source Life Cycle and Sustainability Assessment software. https://www.openlca.org/."

[22] E. Moreno-Ruiz *et al.*, " Documentation of changes implemented in ecoinvent database v3.6. ecoinvent Association," Zürich, Switzerland, 2019.

[23] "The World Energy Absorption Chillers Europe Ltd," *https://www.worldenergyeurope.eu/index.html*.

[24] B. O. Ayugi and G. Tan, "Recent trends of surface air temperatures over Kenya from 1971 to 2010," *Meteorology and Atmospheric Physics*, vol. 131, no. 5, pp. 1401–1413, Oct. 2019, doi: 10.1007/s00703-018-0644-z.

[25] S. M. S. Mahmoudi and M. Akbari Kordlar, "A new flexible geothermal based cogeneration system producing power and refrigeration," *Renew Energy*, vol. 123, pp. 499–512, Aug. 2018, doi: 10.1016/j.renene.2018.02.060.

[26] J. A. Evans *et al.*, "Specific energy consumption values for various refrigerated food cold stores," *Energy Build*, vol. 74, pp. 141–151, May 2014, doi: 10.1016/j.enbuild.2013.11.075.

[27] M. El Haj Assad *et al.*, "Space cooling using geothermal single-effect water/lithium bromide absorption chiller," *Energy Sci Eng*, vol. 9, no. 10, pp. 1747–1760, Oct. 2021, doi: 10.1002/ese3.946.

[28] J. A. Evans *et al.*, "Specific energy consumption values for various refrigerated food cold stores," *Energy Build*, vol. 74, pp. 141–151, May 2014, doi: 10.1016/j.enbuild.2013.11.075.